Transactions on Engineering Sciences vol 25, © 1999 WIT Press, www.witpress.com, ISSN 1743-3533

Effect of residual stress profile on hydrogen embrittlement susceptibility of prestressing steel

J. Toribio, V. Kharin
Department of Materials Science, University of La Coruña
ETSI Caminos, Campus de Elviña, 15192 La Coruña, Spain
EMail: kharin@udc.es

Abstract

A model of hydrogen induced fracture controlled by stress-strain assisted diffusion of hydrogen in metal is proposed and applied to predict time to failure of prestressing steel wires in a hydrogenous environment with different residual stress profiles introduced by surface rolling process.

1 Introduction

Steel wires are used for concrete structures prestressing, a powerful civil engineering technique aiming to introduce desirable stresses and counterbalance undesirable ones so that the prestressing and service loading will produce stresses within specified limits [1]. Prestressing wires are usually made of eutectoid pearlitic steel heavily cold drawn to create elevated tensile properties. These wires, once subjected to high service stresses, remain such forever, obviously in hostile environments, e.g. due to atmospheric humidity. All that makes them sensible to the presence of surface cracks, in particular those of stress corrosion origin. Stress corrosion cracking of prestressing steel has been the subject of extensive studies which substantiated important role of the hydrogen induced fracture (HIF) in deterioration of reinforced concrete structures [2]. To evaluate the susceptibility of prestressing steels to stress corrosion cracking in general, and to HIF in particular, the International Federation for Prestressing (FIP) adopted the Ammonium Thiocyanate Test (ATT) for steel control [3]. However, despite being in use as a standard test method, it does not reveal how HIF goes on in prestressing steel wires and the roles of various manufacturing and service factors. To this end, contributions to a better interpretation of the ATT and understanding of hydrogen embrittlement development in prestressing steel are welcome to gain the capability of monitoring and improving the steel wire performance in hostile environments.

Residual stresses introduced by various manufacturing operations (machining, joining, heat-treating) and surface treatments (rolling, shot-peening, etc.) are known to be capable of influencing components strength and life [4]. With regard to the hydrogen embrittlement of prestressing steel wires, the importance of the residual stresses produced by rolling process has been demonstrated in terms of the wire lives in ATT solution [5]. In the particular case of HIF, the role of the residual stresses is potentially twofold. The first, their mechanical action associated with *the magnitude* of residual stresses is additive to the applied loading stresses [4]. In addition, heterogeneous residual stress fields inluence the hydrogen transportation rate towards prospective rupture sites in the wire by stress-assisted diffusion governed by *the gradient* of the hydrostatic component of stress [6]. Moreover, the facts that residual stresses are produced by inhomogeneous plastic deformation [4] and that this latter itself affects hydrogen diffusion in deformed metals too [7,8], plastic strains caused by surface treatment must be also taken into account as factors affecting the HIF susceptibility of wires.

Previous research [6] dealt with a quantitative relationship between the behaviour of prestressing wires under HIF conditions and the residual stresses levels, but a detailed analysis of the influence of *real* residual stress profiles caused by different regimes of surface rolling on the HIF susceptibility of cold drawn prestressing steel wires has not been performed. In this paper, the earlier developed computer model [6] is advanced and applied to analyze the influence of the residual stress-and-strain profiles after surface rolling on the hydrogen embrittlement susceptibility of cold drawn prestressing steel wires in FIP tests.

2 Background Theory

In general, HIF depends on the amount of hydrogen in prospective fracture sites in metal so that rupture events are associated with a critical combination of the responsible stress-strain field characteristics and hydrogen concentration C over a relevant material scale x_c (cell, "grain", or domain of interest) [7,8]. HIF advances by hydrogen-assisted nucleation of a (micro)crack in the site of the locally worst concentration-stress-strain triple which may be resolved to define the critical concentration of hydrogen as follows:

$$C_{cr} = C_{cr}\,(\sigma_i, \varepsilon_{pi}), \tag{1}$$

where $\sigma_i = \sigma_i(x)$ and $\varepsilon_{pi} = \varepsilon_{pi}(x)$ represent, respectively, the three principal components of stresses and plastic strains (i = 1,2,3) in a material point x. In particular cases of predominantly stress- or strain-controlled HIF, C_{cr} will be related to the corresponding single governing mechanical variable.

Hydrogen from corrosive environment penetrates into the metal and is accumulated in prospective fracture sites until its concentration C(x,t) attains the critical level after a certain time t, and this is when rupture event occurs. The criterion to determine fracture time t_f takes then the form:

$$C(x_c, t_f) = C_{cr}\,(x_c), \tag{2}$$

where a definite fracture locus x_c must be specified.

Although hydrogen transportation towards damage sites comprises several consecutive stages [6-8], the slowest one which controls fracture time is often hydrogen diffusion in metal. In particular, this is considered to be the case under electrochemical hydrogenation, such as during ATT [6,9]. Diffusion in metals proceeds towards maximal entropy which corresponds to uniform distribution of a given amount of a specie, represented by its concentration C, over available occupation sites which density is characterised by the solubility factor K_S. This latter depends on metal lattice dilatation induced by hydrostatic stress σ, and on the amount of lattice imperfections (traps for hydrogen [10]) related to equivalent plastic strain ε_p, which may be expressed as follows [7-9]:

$$K_S(\sigma,\varepsilon_p) = K_{S\varepsilon}(\varepsilon_p)\exp(\Omega\sigma) \quad \text{with } \Omega = \frac{V_H}{RT}, \tag{3}$$

where $K_{S\varepsilon}$ is the strain-dependent component of solubility, V_H is the partial molar volume of hydrogen in metal, R the universal gas constant, and T the absolute temperature. This leads to the stress-strain affected diffusion flux [7-9]:

$$\mathbf{J} = -D(\varepsilon_p)\left\{\nabla C - C\left[\Omega\nabla\sigma + \frac{\nabla K_{S\varepsilon}(\varepsilon_p)}{K_{S\varepsilon}(\varepsilon_p)}\right]\right\}, \tag{4}$$

where D is the diffusion coefficient of hydrogen in metal which characterises the specie mobility and depends on lattice trap density, and this way on ε_p. Mass balance then gives the diffusion equation in terms of concentration in the form:

$$\frac{\partial C}{\partial t} = -\operatorname{div}\mathbf{J}. \tag{5}$$

Hydrogen entry into metal, i.e. the boundary condition for diffusion, consistent with the role of diffusion as the rate-controlling step [8,9] and with the solubility expression (3), corresponds to the equilibrium between its environmental activity and concentration within metal at the entry surface Γ:

$$C(\Gamma,t) = C_\Gamma \text{ with } C_\Gamma = C_e K_{S\varepsilon}(\varepsilon_p(\Gamma))\exp(\Omega\sigma(\Gamma)), \tag{6}$$

where C_e is the equilibrium concentration of hydrogen in virgin material under given environmental conditions [8,9].

3 Study of HIF in Prestressing Steel Wires

3.1 Test Description

According to the FIP proposal [3], the ATT for hydrogen susceptibility evaluation of prestressing steels is performed by sustained loading of smooth

round wires submerged in 20-wt.% aqueous solution of ammonium thiocyanate (NH_4SCN) and monitoring the time to fracture t_f vs. applied stress σ_{ap}.

The tests to be analysed [5,6] were performed with prestressing steel wires of eutectoid high-strength steel which was cold drawn from a rod of initial diameter d_0 = 12 mm to achieve the wire diameter d = 7 mm, and afterwards submitted to stress-relieve heat treatment with cooling in oil. The 0,2%-offset yield stress is $\sigma_{0.2}$ = 1435 MPa and the fracture toughness in inert environment K_{IC} = 98 MPa $m^{1/2}$ [5,6]. A series of samples were tested in the as-received condition (specimens C0), others were subjected to surface treatment by rolling process under loads of 80 and 260 N (specimens C8 and C26 respectively) [5].

3.2 Distributions of Residual Stresses and Strains

To analyse the role of surface treatments on the hydrogen embrittlement susceptibility of the wires, the data of X-ray diffraction measurements of the residual stresses and plastic strains inhomogeneity by Campos and Elices [5] are used. These results are available for the depths from the specimen surface up to 500 μm and mostly for the sole axial component σ_{zR} of the residual stresses, whereas analysis of hydrogen diffusion requires hydrostatic stress distributions along the wire radius $0 \le r \le a = d/2$. To fill in this deficiency, the reconstruction of the residual stresses was performed basing on these limited X-ray measurements for σ_{zR} stress in the wires under consideration [5]. Limiting to the axisymmetric problem in cylindrical coordinates (r,θ,z), the hoop residual stress $\sigma_{\theta R}(r)$ for the measured depths was estimated according to the available $\sigma_{zR}(r)$-distributions using some similitude hypothesis derived from the analysis of the more representative sets of σ_z and σ_θ measurements in similar cases [4,5]. Then, for greater depths up to the wire axis, all stress distributions were extrapolated by quadratic parabolas satisfying the global equilibrium conditions over respective transverse and axial cross-sections. The radial stress $\sigma_{rR}(r)$ was evaluated from the reconstructed $\sigma_\theta(r)$ distribution according to the equilibrium equation which here reduces to the following:

$$\frac{d\,(r\,\sigma_{rR})}{d\,r} = \sigma_{\theta R}(r). \tag{7}$$

Hydrostatic residual stresses $\sigma_R = (\sigma_{rR} + \sigma_{\theta R} + \sigma_{zR})/3$ obtained this way are presented in Fig. 1. It is seen that the rolling process introduces severe inhomogeneity of residual stresses (samples C8 and C26) in contrast to relatively uniform distributions after drawing only (sample C0).

These nonuniform residual stresses are the consequences of the inhomogeneous near-surface plastic deformation due to rolling. The variation of the X-ray diffraction peak width was suggested as an indicator of the plastic strains inhomogeneity [5]. According to the measurements [5], plastic strain distribution after cold drawing without rolling is relatively homogeneous. Using the plastic incompressibility condition and the rod diameter reduction by cold

drawing, the corresponding background level of the equivalent plastic strain in wires C0 may be estimated as $\varepsilon_{p0} = 2\ln(d/d_0)$. Then, for the rolled wires C8 and C26 the plastic strains were approximated from the corresponding X-ray data [5] by piece-wise linear distributions shown in Fig. 1.

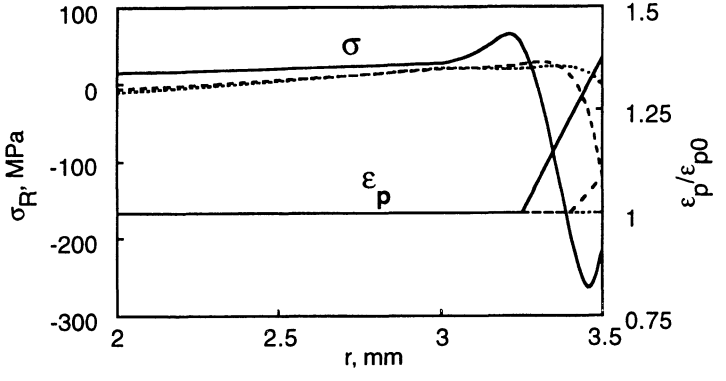

Figure 1: Residual hydrostatic stress and plastic strain profiles in cold drawn wires C0 (dotted lines), C8 (dashed lines) and C26 (solid lines).

3.3 Model of Hydrogen Induced Fracture

With regard to fracture, the adopted model is basically the same as that proposed and substantiated in the paper [6]. The HIF criterion (2) is particularised so that fracture initiates —and a crack of depth x_c is assumed to arise— when over a critical initiation scale x_c the average hydrogen concentration

$$\langle C(r,t)\rangle_{xc} = \frac{1}{x_c}\int_{r-x_c}^{a} C(r,t)\,dr \tag{8}$$

attains the level $C_{cr}(\langle\sigma_{z,ef}\rangle_{xc})$, where effective crack opening stress $\sigma_{z,ef}$ is the sum of the applied and residual axial stresses, $\sigma_{z,ef} = \sigma_{ap} + \sigma_{zR}$, and its average value $\langle\sigma_{z,ef}\rangle_{xc}$ is defined analogously to eqn (8). The subcritical crack growth phase from the size x_c to terminal rupture is neglected, which for high strength wires was shown [6] to agree with experiments. Accordingly, the fracture condition is expressed through the stress intensity factor:

$$K_I(x_c,\sigma_{z,ef}) = K_{IHAC}, \tag{9}$$

where K_{IHAC} is the threshold stress intensity factor for hydrogen assisted cracking under given environmental conditions.

Fracture embryo is assumed to be a surface semi-elliptical crack with depth-to-width aspect ratio of 0.2. For arbitrary $\sigma_{z,ef}(r)$, stress intensity factor values may be calculated using the weight function method [11]. However, for all

considered $\sigma_{ZR}(r)$-distributions being here similar to the $\sigma_R(r)$-paths shown in Fig. 1, in a relevant range of crack depths it was confirmed that, with an error less than 5%, K_I may be evaluated by means of the following formula [6]:

$$K_I = 0.94 \langle\sigma_{z,ef}\rangle_{x_c} \sqrt{\pi x_c}. \tag{10}$$

Then, from eqns (9) and (10), the critical scale for HIF is:

$$x_c = \frac{1}{\pi}\left[\frac{K_{IHAC}}{0.94\langle\sigma_{z,ef}\rangle_{xc}}\right]^2. \tag{11}$$

Finally, the criterion for HIF is the averaging of the eqn (2) over the fracture scale x_c similarly to eqn (8), so that the equation to predict the wire life t_f in ATT solution takes the form:

$$\langle C(r,t_f)\rangle_{xc} = C_{cr}(\langle\sigma_{z,ef}\rangle_{xc}). \tag{12}$$

This allows one to calculate t_f on the basis of the solution of the problem of stress-strain assisted hydrogen diffusion of in a loaded wire in the course of ATT.

4 Wire Life Prediction

The model presented in the previous section points out the way to elucidate the role of residual stress profiles (and of respective surface treatments) in HIF of wires, and to predict the time to fracture of prestressing steel in hydrogenating environment. To implement the model, a set of material properties must be specified. On the basis of the available experimental knowledge, the input data were chosen as follows.

To compare model simulations with experiments [5,6], the temperature was fixed T = 323 K. The partial molar volume for steels is fairly constant, $V_H = 2$ cm^3/mol [6,10]. With regard to the diffusion coefficient, wide dispersion of the measured data is proper at ambient temperatures for nominally the same metals, as well as the hydrogen solubility data are also rather ambiguous, all of them being very sensitive to paltry peculiarities of alloy composition and microstructure [10,12]. Quantitative information about their dependence on plastic strain is rare for most commercial alloys. Nevertheless, as reasonable estimations, the following may be accepted (cf. [6,12,13]):

$$D(\varepsilon_p) = D_0 \exp(-\alpha\varepsilon_p) \text{ with } \alpha = 2.9, \tag{13}$$

$$K_{S\varepsilon}(\varepsilon_p) = 1 + \beta\varepsilon_p \text{ with } \beta = 4, \tag{14}$$

where D_0 is the diffusion coefficient in "strain-free" (as-received, before cold drawing) steel rod, $D_0 = 3{\cdot}10^{-12}$ m^2/s at given temperature. Finally, $K_{IHAC} = 0.27K_{IC}$ [6] for commercial prestressing steel in the ATT solution.

To evaluate the left-hand quantity of the eqn (12), evolution of hydrogen concentration in a sample must be determined by solution of the problem of stress-strain assisted diffusion (4)-(6) in terms of dimensionless concentration $C(r,t)/C_\Gamma$. Zero initial condition is taken here, $C(r,0) = 0$.

Numerical analysis of axisymmetrical stress-strain affected diffusion was implemented basically as described elsewhere [14] following the standard weighted residual process to built up a finite-element approximation of the initial-boundary value problem (5)-(6). In brief, applying the Galerkin process for the continuum discretized into a finite elements, the same shape functions $\{W_m(r);\ m = 1,2,...,M\}$, M being the number of nodes in the mesh, served as trial and weighting functions, and also were used to approximate stress distributions $\sigma_R(r)$ (Fig. 1), diffusion coefficient and solubility (13)-(14) dependent on plastic strain $\varepsilon_p(r)$ also shown in Fig. 1. The weak form of the weighted residual statement of the problem rendered the system of equations with respect to the nodal concentration values to solve which the unconditionally stable Galerkin scheme of time-domain integration was employed. Simulations were performed using linear trial functions W_m. Nonuniform spatial discretisation was employed to fit steep gradients of stress (see Fig. 1) and concentration. The smallest elements were about 5 μm length.

For all three residual stress-strain field profiles, results of the diffusion computations together with equilibrium concentration distribution at $t \to \infty$ given by known steady-state solution of the problem, $C_\infty(r)/C_e = K_S(\sigma(r),\varepsilon_p(r))$, cf. [7-9], are presented in Fig. 2. The effect of stress-strain field induced by rolling is notable mostly in the near surface zone where interaction of stress- and strain-controlled solubility terms (cf. eqns (3) and (14), and Fig. 1) causes respective concentration peaks. Closer to the wire axis, slight concentration delay, being increasing with more intense rolling, due to the local decrease of diffusivity D by elevated plastic strain (traps density), cf. eqn (13) and Fig. 1.

To predict theoretically wire lives in terms of plots of applied stress vs. time to fracture, critical concentration values C_{cr} for respective wires were calculated according to the presented HIF model after diffusion simulations as the averages (8) of the obtained solutions $C(r,t)$ at the experimental times of fracture in ATT solution $t = t_f$ available for all three wires at a single load level of σ_{ap} = 1346 MPa [5] (shown by squares in Fig. 3). Then, the entire $\sigma_{ap}(t_f)$-curves were reconstructed according to eqn (12) from the results of the diffusion calculations and these C_{cr} values, taken to be constants for the respective wires C0, C8 and C26 in a relatively narrow range of the applied stress under consideration. These curves are displayed in Fig. 3. The experimental data [6] obtained at various load levels for a steel nominally the same as C0 —but from another commercial stock— are also shown there.

The presented HIF model seems to be able to give trustworthy predictions of prestressing steel lives under hydrogen embrittlement with account for the role of residual stresses induced by surface treatment processes. It explains their

effect by the influence on the stress-strain assisted diffusion of hydrogen towards rupture sites.

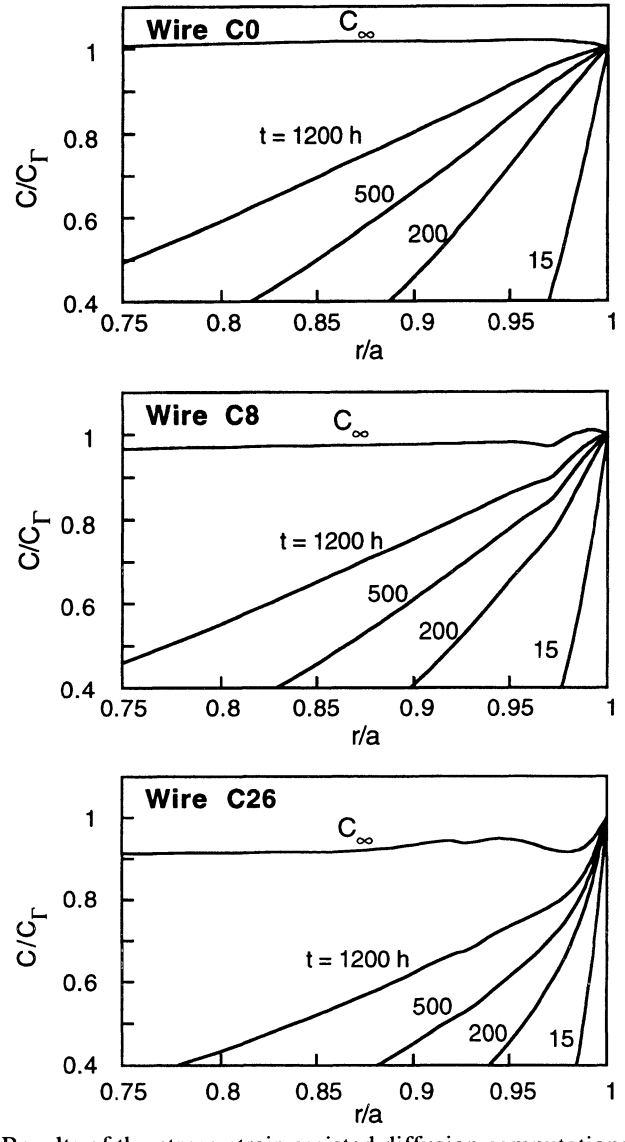

Figure 2: Results of the stress-strain assisted diffusion computations for residual stress and plastic strain distributions in the wires C0, C8 and C26.

Presented theory may be employed, in particular, to reduce the terms and costs of the experiments to evaluate the susceptibility of wires to hydrogen embrittlement by performing only single and short-term tests at elevated load levels, estimating the critical concentration C_{cr}, and reconstructing the entire

curves σ_{ap} vs. t_f as described before. These theoretical curves must provide safe life estimation for lower load levels. This is because at lower σ_{ap} actual critical concentrations may be only higher than C_{cr} value theoretically estimated for elevated load, and so the actual time to reach critical condition can be longer than theoretical prediction. However, adequate estimation of the diffusion coefficient D is crucial for the reliability of these predictions.

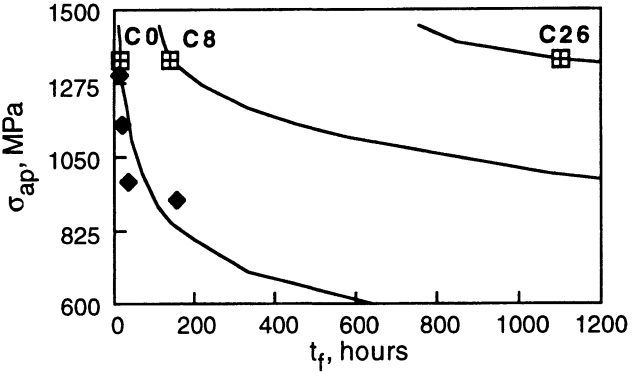

Figure 3: Theoretical predictions of prestressing steel lifes t_f vs. applied stress σ_{ap} in the ATT solution (curves for respective wires C0, C8 and C26 as indicated) and respective source data of single experiments [5] (squares); filled rhombs represent experimental data for a steel similar to C0 but obtained from a different commercial stock [6].

5 Conclusions

A model was developed to predict the life of high strength steel wires in ATT solution based on the theory of stress-strain affected hydrogen diffusion and hydrogen induced fracture criterion.

The genuine residual stress and plastic strain profiles in the prestressing steels were reconstructed on the basis of X-ray diffraction measurements, and their effects on hydrogen embrittlement susceptibility were calculated according to the proposed model. Fair predictions of the available experimental results about time to failure in ATT solution were obtained.

Proposed computational model seems to be a promising tool to predict the lives of prestressing steel wires under hydrogen embrittlement conditions on the basis of reduced testing, and to account for various residual stress an strain profiles induced by surface treatments.

Acknowledgements

This work was funded by the Spanish CICYT (Grant MAT97-0442) and *Xunta de Galicia* (Grants XUGA 11801B95 and XUGA 11802B97). One of the authors (VKh) is indebted to *Xunta de Galicia* for supporting his stay as a visiting scientist at the University of La Coruña (Spain).

References

1. Valiente, A. & Elices, M., Premature failure of prestressed steel bars, *Engng. Failure Anal.*, **5**, pp. 219-227, 1998.

2. Bergsma, F., Boon, J.W. & Etienne, C.F., Détermination de la sensibilité des aciers précontrains à la fragilisation par l'hydrogène, *Rev. métalurgie*, **75**, pp. 153-164, 1978.

3. FIP-78. *Stress Corrosion Test. Stress Corrosion Cracking Resistance for Prestressing Tendons*. Techn. Rep. No. 5. FIP, Wexham Springs, Slough, UK, 1981.

4. Macherauch, E., Introduction to residual stress, *Advances in Surface Treatment*, Vol. 4, Oxford, pp. 1-36, 1987.

5. Campos, J.M. & Elices, M., Tensiones residuales internas en alambres trefilados, *Anales Mec. Fractura*, **4**, pp. 143-157, 1987.

6. Toribio, J. & Elices, M., Influence of residual stresses on hydrogen embrittlement susceptibility of prestressing steels, *Int. J. Solids Struct.*, **28**, pp. 791-803, 1991.

7. Toribio, J. & Kharin, V., Evaluation of hydrogen assisted cracking: the meaning and significance of the fracture mechanics approach, *Nucl. Engng. and Des.*, **182**, pp. 149-163, 1998.

8. Toribio, J. & Kharin, V., The effect of history on hydrogen assisted cracking: 1. Coupling of hydrogenation and crack growth, *Int. J. Fracture*, **88**, pp. 233-245, 1997 (1998).

9. Toribio, J. & Kharin, V., K-dominance condition in hydrogen assisted cracking: the role of the far field, *Fatigue Fract. Engng. Mater. Struct.*, **20**, pp. 729-745, 1997.

10. Hirth, J.P., Effects of hydrogen on the properties of iron and steel, *Met. Trans.*, **11A**, pp. 861-890, 1980.

11. Fett, T. & Munz, D., *Stress Intensity Factors and Weight Functions*, Computational Mechanics Publications, Southampton-Boston, 1997.

12. Coe, F.R. & Moreton, J., Diffusion of hydrogen in low-alloy steel, *J. Iron and Steel Inst.*, **204**, pp. 366-370, 1966.

13. Astiz, M.A., Álvarez, J.A. & Guitiérrez-Solana, F., Modelo numérico para analizar el efecto del hidrógeno sobre los procesos de fisuración dúctil, *Anales Mec. Fractura,* **15**, pp. 79-84, 1998.

14. Toribio, J. & Kharin, V., Role of fatigue crack closure stresses in hydrogen assisted cracking, *Advances in Fatigue Crack Closure Measurement and Analysis. Second Volume*, ASTM STP 1343, Philadelphia, PA (In press).